

Crystal structure of human ERK2 complexed with a pyrazolo[3,4-*c*]pyridazine derivative

Takayoshi Kinoshita,^{a,*} Masaichi Warizaya,^a Makoto Ohori,^a Kentaro Sato,^b Masahiro Neya^a and Takashi Fujii^a

^aExploratory Research Laboratories, Fujisawa Pharmaceutical Co., Ltd, 5-2-3 Tokodai, Tsukuba, Ibaraki 300-2698, Japan

^bMedicinal Chemistry Research Laboratories, Fujisawa Pharmaceutical Co., Ltd, 5-2-3 Tokodai, Tsukuba, Ibaraki 300-2698, Japan

Received 10 March 2005; revised 8 September 2005; accepted 21 September 2005

Available online 18 October 2005

Abstract—A series of pyrazolopyridazine compounds were briefly investigated as ERK2 inhibitors. The crystal structure of ERK2 complexed with an allyl derivative was determined. The compound induces structural change including movement of the glycine-rich loop and peptide flip between Met108–Glu109. As a result, the newly formed subsite can recognize small hydrophobic substituents but not hydrophilic ones.

© 2005 Elsevier Ltd. All rights reserved.

Extracellular signal-regulated kinase 2 (ERK2, E.C. 2.7.1.37) is a member of the Ras/Raf/MEK1(or MEK2)/ERK1(or ERK2) mitogen-activated protein kinase (MAPK) signaling pathways. These pathways contribute to the coordination and regulation of cell growth and differentiation in response to extracellular stimulation.¹ They function as an integral step in the formation, progression, and survival of tumors, in addition to being intracellular mediators in signaling aberrations in many inflammatory processes.² Based on experimental evidence, the MAPK signaling pathways represent an attractive target for pharmacological intervention in proliferative and inflammatory diseases.³

Recently, we discovered that a 1*H*-pyrazolo[3,4-*c*]pyridazine derivative **1** acted as a potent ERK2 inhibitor that dose-dependently depressed AP-1-dependent transcription induced by TGFβ1, as an inflammatory mediator.⁴ Compound **1** showed ATP-competitive inhibition in a Lineweaver–Burk analysis and was the first compound with high selectivity toward many other kinases. Among known ERK2 inhibitors such as olomoucine and 5-indotubercidin, which have low selectivity. The compound is useful as a tool to elucidate the roles of ERK

in a variety of cellular events. X-ray analysis⁴ confirmed that it bound to the ATP binding site of the enzyme with a novel binding mode. The phenyl moiety and the pyrazolopyridazine moiety bind to the bottom of the active site, which is structurally rigid. On the other hand, the pyrazolopyridazine moiety binds to the entrance region of the active site, which consists of structurally flexible loops.

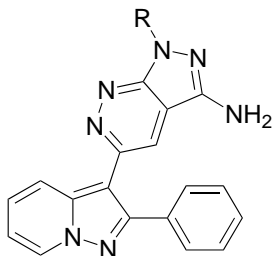
Kinases, including ERK2, have a common architecture, and contain an ATP binding site consisting of flexible loops known as a glycine-rich loop and an activation loop. The glycine-rich loop has various conformations according to the binding of different inhibitors. The flexibility allows recognition of a variety of structural compounds. The glycine-rich loop in the **1**/ERK2 complex is different from those in the previously reported structures.⁵

For a brief investigation on the structural flexibility of the glycine-rich loop, compounds **2–4**, with various substituents at the 1-position of the pyrazolopyridazine ring, were synthesized.⁶ The respective inhibitory activities⁷ are shown in Table 1.

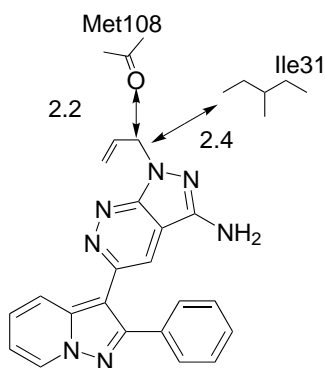
Compounds **2** and **3** have inhibitory activity higher than that of **1**, although activity reduction would be expected due to the steric hindrance between these compounds and the protein (Fig. 1). The substituents at the 1*H* position would obstruct the Cδ atom of Ile31 and the carbonyl group of Met108 if the structure in the

Keywords: ERK2; X-ray; Structural change.

* Corresponding author. Present address: Department of Biological Science, Graduate School of Science, Osaka Prefecture University, Gakuencho 1-1, Sakai, Osaka 599-8531, Japan. Tel.: +81 72 2549819; fax: +81 72 2549935; e-mail: kinotk@b.s.osakafu-u.ac.jp

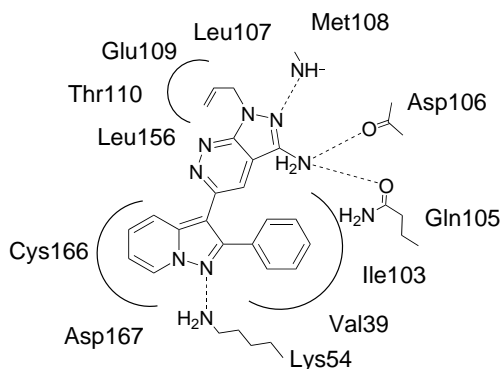
Table 1. Classical complement inhibition for compounds 1–4


Compound	R	IC ₅₀ (μM)
1	H	1.9
2	Me	1.4
3	CH ₂ CH=CH ₂	0.56
4	CH ₂ CH ₂ OH	5.1

**Figure 1.** Steric hindrance when there is no structural change. Distances are shown in Å. The model of compound 3 was calculated based upon the coordinates of compound 1 in the 1/ERK2 complex and was superposed onto the ERK2 protein in the 1/ERK2 complex.

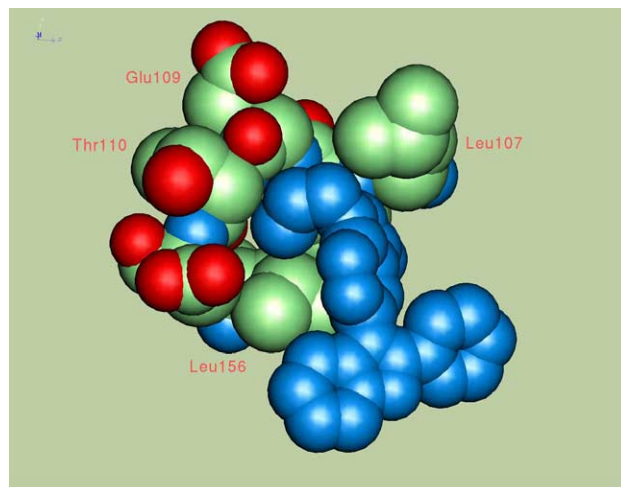
1/ERK2 complex were rigid. That is, conformational change of the protein may occur. Alternatively, a structural difference may be brought about by the interaction mode.

The crystal structure of the 3/ERK2 complex⁸ reveals that 3 binds to the protein in the same manner as 1, except around the allyl moiety (Fig. 2). All interactions of the 1/ERK2 complex are conserved in the 3/ERK2

**Figure 2.** Interaction pattern of the X-ray structure.

complex. The amino group forms a hydrogen bond with the carbonyl of Asp106 and the amide carbonyl of Gln105. The N2 atom of the pyrazolopyridazine ring interacts with the NH of Met108. This interaction is important for the recognition of various inhibitors by their respective kinases.⁹ The N2 atom of the pyrazolopyridine ring interacts with the Lys54. The phenyl group binds in the hydrophobic subsite consisting of Val39, Ile103 and the methylene chains of Lys54 and Gln105. These portions of the protein are rigid in the 1/ERK2 and 3/ERK2 complexes. On the other hand, the allyl group fits well into the newly formed hydrophobic subsite consisting of Leu107, Leu156, and the peptide backbone of Glu109 and Thr110 (Fig. 3). The methylene part of the allyl group has a hydrophobic interaction with Leu107. The vinyl group also has a hydrophobic interaction with Leu156 and has van der Waals contacts with the peptide backbone of Glu109 and Thr110.

As a result, the allyl group of the inhibitor moves the Ile31 residue and the carbonyl group of Met108 away from this position in the 1/ERK2 complex (Fig. 4). The Cα atom of Ile31 in the glycine-rich loop is pushed out from the position it occupies in 1/ERK2 by 2.0 Å. The whole of the glycine-rich loop is moved out with the Ile31, but this movement has no influence on the molecular recognition pattern. The carbonyl group of Met108 is directed to the opposite side of the allyl group, but the Cα atoms of both ends of the peptide bond are fixed in the two complexes. That is, the peptide flip between Met108 and Glu109 occurs as observed in p38 mitogen-activated protein kinase complexed with a quinazolinone inhibitor.¹⁰ Furthermore, the peptide flip in the p38 kinase occurs between Met109 and Gly110, and the large residue makes the peptide flip energetically unfavorable, based on the mutational investigations at Gly110. In the case of the 3/ERK2 complex, the peptide flip occurs even though the peptide consists of large residues. Overall, two disadvantageous factors in the allyl group binding are settled by this motion. This structural

**Figure 3.** Structure around the allyl group in the 3/ERK2 complex (van der Waals sphere models).

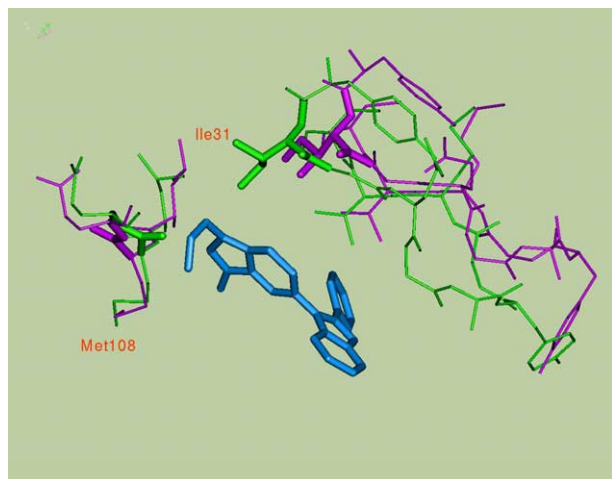


Figure 4. Conformational change induced by compound **3**. The protein structures of the **1**/ERK2 and **3**/ERK2 complexes are shown as green and magenta stick models, respectively. Ile31, the carbonyl group of Met108, and compound **3** (blue) are highlighted by bold sticks.

difference between the **1**/ERK2 and **3**/ERK2 complexes is not an artifact due to crystal packing, but is a result of inhibitor-induced conformational change, since both conformations are observed in the same crystal systems.

Compound **4** has inhibitory activity that is 9 times lower than that of **3**, although both have similar sized substituents at the 1-position of the pyrazolopyridazine frame. The structure of the **3**/ERK2 complex was considered in order to determine a reason for this, and the hydroxyl group may be unsuitable for a hydrophobic environment. Furthermore, the hydrophobic interaction with the peptide backbone may be important for the binding of **3**. The methyl group of **2** cannot make this interaction, but can make a hydrophobic interaction with Leu107. Therefore, compound **2** has activity higher than that of compound **1** and has activity lower than that of compound **3**.

In conclusion, we have briefly investigated the structural properties of the substituent of the pyrazolopyridazine ring. The crystal structures of the **3**/ERK2 complex as well as the **1**/ERK2 complex provide useful insights which could be used in the design of more potent ERK2 inhibitors.

References and notes

- (a) Ahn, N. G.; Seger, R.; Bratlien, R. L.; Diltz, C. D.; Tonks, N. K.; Krebs, E. G. *J. Biol. Chem.* **1991**, *266*, 4220; (b) Zheng, C-F.; Guan, K. *J. Biol. Chem.* **1993**, *268*, 11435; (c) Dhanasekaran, N.; Reddy, P. *Oncogene* **1998**, *17*, 1447; (d) Kolch, W. *Expert Opin. Pharmacother.* **2002**, *3*, 709; (e) Schaeffer, H. J.; Weber, M. J. *Mol. Cell. Biol.* **1999**, *19*, 2435.
- (a) Herrera, R.; Sebolt-Leopold, J. S. *Trends Mol. Med.* **2002**, *8*, S27; (b) Kyriakis, J. M.; Avruch, J. *Physiol. Rev.* **2002**, *81*, 807.
- (a) Dudley, D. T.; Pang, L.; Decker, S. J.; Bridges, A. J.; Saltiel, A. R. *Proc. Natl. Acad. Sci. U.S.A.* **1995**, *92*, 7686; (b) Sebolt-Leopold, J. S.; Dudley, D. T.; Herrera, R.; Becelaere, K. V.; Wiland, A.; Gowan, R. C.; Tecle, H.; Barrett, S. D.; Bridges, A.; Przybranowski, S.; Leopold, W. R.; Saltiel, A. R. *Nat. Med.* **1999**, *5*, 810.
- Ohori, M.; Kinoshita, T.; Okubo, M.; Sato, K.; Yamazaki, A.; Arakawa, H.; Nishimura, S.; Inamura, N.; Nakajima, H.; Neya, M.; Miyake, H.; Fujii, T. *Biochem. Biophys. Res. Commun.* **2005**, *336*, 357, The structure of the **1**/ERK2 complex deposited to the Protein Data Bank (accession code: 1TVO).
- (a) Zhang, F.; Strand, A.; Robbins, D.; Cobb, M. H.; Goldsmith, E. J. *Nature* **1994**, *367*, 704; (b) Wang, Z.; Canagarajah, B. J.; Boehm, J. C.; Kassisa, S.; Cobb, M. H.; Young, P. R.; Abdel-Meguid, S.; Adams, J. L.; Goldsmith, E. J. *Structure* **1998**, *6*, 1117.
- Data for **2**: ^1H NMR (300 MHz, CDCl_3) δ 4.08 (br s, 2H), 4.15 (s, 3H), 6.88 (dd, 1H, $J = 6.2, 6.2$ Hz), 7.24 (dd, 1H, $J = 6.2, 6.2$ Hz), 7.37–7.43 (m, 3H), 7.41 (s, 1H), 8.20 (d, 1H, $J = 7.7$ Hz), 8.54 (d, 1H, $J = 7.7$ Hz). MS(M+1) 342. Data for **3**: ^1H NMR (300 MHz, CDCl_3) δ 4.10 (br s, 2H), 5.15 (d, 1H, $J = 6.6$ Hz), 5.27–5.40 (m, 2H), 6.05–6.19 (m, 1H), 6.89 (dd, 1H, $J = 7.6$ Hz), 7.24 (dd, 1H, $J = 7.6$ Hz), 7.38–7.42 (m, 3H), 7.42 (s, 1H), 7.58–7.64 (m, 2H), 8.24 (d, 1H, $J = 7.8$ Hz), 8.54 (d, 1H, $J = 7.8$ Hz). MS(M+1) 368. Data for **4**: ^1H NMR (300 MHz, CDCl_3) δ 4.13 (t, 2H, $J = 5.8$ Hz), 4.65 (t, 2H, $J = 5.8$ Hz), 6.90 (dd, 1H, $J = 7.4, 7.4$ Hz), 7.27 (1H, $J = 6.2, 6.2$ Hz), 7.38–7.46 (m, 3H), 7.47 (s, 1H), 7.57–7.65 (m, 2H), 8.17 (d, 1H, $J = 7.7$ Hz), 8.54 (d, 1H, $J = 7.7$ Hz). MS(M+1) 372.
- The inhibitory assay is performed by a procedure similar to that described in Ref. 4. Nunc-Immuno MaxiSorp plates (Nalge Nunc International, Rochester, NY) were coated with 20 $\mu\text{g}/\text{ml}$ MBP solution in phosphate-buffered saline (PBS). After washing with PBS containing 0.05% Tween 20 (T-PBS), blocking buffer (T-PBS containing 3% BSA) was added to each well and the wells were incubated for 10 min at room temperature. After washing with T-PBS, compounds **1–4**, ATP, and recombinant ERK2 (Upstate Biotechnology) diluted in assay dilution buffer (20 mM MOPS, pH 7.2, 25 mM β -glycerol phosphate, 5 mM EGTA, 1 mM sodium orthovanadate, 1 mM dithiothreitol, and 50 $\mu\text{g}/\text{ml}$ BSA) were added to each well. Vehicle groups (containing 0.1% DMSO) and kinase withdrawal groups were used for the control and basal determinations, respectively. After incubation for 1 h at room temperature, plates were washed twice with T-PBS. Anti-phospho MBP antibody (0.2 $\mu\text{g}/\text{ml}$) was added to each well and incubated for 1 h at room temperature. After washing, anti-mouse HRP-conjugated polyclonal antibodies were added and incubated for 30 min. Super Signal kit (Pierce Biochemicals) was used for the measurement of HRP activity as per the manufacturer's instructions. Prism4.0 (GraphPad Software Inc., San Diego, CA) was used for Lineweaver–Burk plot analysis and IC_{50} determinations.
- Crystallography of **3**/ERK2. Cocrystals of the human ERK2 were obtained using procedures similar to those previously described.⁴ In this study, 100 mM Bis–Tris, pH 6.5, 0.2 M ammonium sulfate, and 35% (v/v) PEG5000 were used as precipitants. X-ray diffraction data were collected from this $P2_1$ form: $a = 48.60$ Å, $b = 68.54$ Å, $c = 59.83$ Å, and $\beta = 110.3^\circ$, at SP-ring8 beamline 32B2. The wavelength was 1.0 Å and the crystal-to-detector length was 400 mm. Data resolution is from 45.6 to 2.5 Å; 48,902 observations were scaled and merged into 12,864 unique reflections using Crystal Clear (RIGAKU). The overall R -merge (I) is 9.9%, the ratio $I/\sigma(I)$ is 6.4, and the

data are 99.9% complete. Corresponding values for the high-resolution data shell (2.59–2.50 Å) are 19.0%, 3.8%, and 99.8%, respectively. The structure of the complex was solved and refined using these data, programs AMoRe¹¹ and X-PLOR (Accelrys), and the protein model 1TVO from the Protein Data Bank.⁴ The conventional and free R-factors after refinement are 24.9% and 29.2%. The rms deviations between model and ideal bond distances, bond angles, dihedral angles, and improper angles are 0.007 Å, 1.7°, 22.3°, and 1.07°, respectively. Several amino acids, eight amino acids as the cloning artifact, seven amino

acids from the N-terminus, and three amino acids from the C-terminus, were omitted from the final model because of ambiguous or discontinuous electron density for the corresponding regions. The model coordinates have been deposited in the Protein Data Bank with the code 1WZY.

9. Cherry, M.; Williams, D. H. *Curr. Med. Chem.* **2004**, *11*, 663.
10. Fitzgerald, C. E.; Patel, S. B.; Becker, J. W.; Cameron, P. M.; Zaller, D.; Pikounis, V. B.; O'Keefe, S. J.; Scapin, G. *Nat. Struct. Biol.* **2003**, *10*, 764.
11. Navaza, J. *Acta. Crystallogr.* **1993**, *D49*, 588.